

ORIGINAL ARTICLE

Polymeric photonic molecule super-mode lasers on silicon

Tobias Grossmann^{1,2}, Tobias Wienhold², Uwe Bog², Torsten Beck¹, Christian Friedmann³, Heinz Kalt¹ and Timo Mappes^{2,4}

Optically coupled microcavities have emerged as photonic structures with promising properties for investigation of fundamental science as well as for applications. We report on the fabrication and spatially resolved spectroscopy of on-chip photonic molecule (PM) lasers consisting of two coupled, dye-doped polymeric microdisks on a silicon substrate. We investigate the fundamental lasing properties with focus on the spatial distribution of modes, the coupling dependent suppression of lasing modes, and in particular the application-oriented operation of these devices in aqueous environments. By depositing an additional polymer layer onto the lithographically structured cavities made of dye-doped poly(methyl methacrylate), coupling-gap widths below 150 nm with aspect ratios of the micro-/nanostucture exceeding 9 : 1 are achieved. This enables strong optical coupling at visible wavelengths despite relatively small resonator radii of 25 μm . The lasing properties of dye-doped PMs are investigated using spatially resolved micro-photoluminescence ($\mu\text{-PL}$) spectroscopy. This technique allows for the direct imaging of whispering-gallery modes (WGMs) in the photonic molecules. For subwavelength coupling gaps, we observe lasing from delocalized eigenstates of the PMs (termed in the following as super-modes). Using size-mismatched cavities, the lasing mode suppression for different coupling-gap widths is investigated. We further demonstrate single-mode lasing operation in aqueous environments with PMs, which are realized on a low-cost, polymer-on-silicon platform.

Light: Science & Applications (2013) 2, e82; doi:10.1038/lsa.2013.38; published online 24 May 2013

Keywords: microcavity lasers; photonic molecules; visible lasers; whispering-gallery modes

INTRODUCTION

Optically coupled microcavities are attractive devices for the investigation of fundamental physics, e.g., quantum optics,^{1–4} as well as for applications, such as sensing^{5–9} or telecommunications.^{10,11} Two or more coupled microresonators are often referred to as photonic molecule (PM), due to the formation of optical bonding and antibonding modes in analogy to the electronic states in molecules formed by atoms.¹² In comparison to single microcavities PMs provide additional degrees of freedom to tailor the optical density of states and the spatial distribution of modes. This makes PMs especially attractive for lasing devices, as coupling of size-mismatched resonators can lead to suppression of laser modes, which has been used for the demonstration of optofluidic- and capillary-based single mode lasers.^{13,14} Although the coupling between two resonators is known to play a major role for the suppression of laser modes,¹³ so far no detailed experimental studies have been performed to investigate the localization of lasing whispering-gallery modes in PMs and the effect of coupling on the localization as well as on the suppression of lasing modes.

In addition to lasing devices, PMs provide promising prospects for applications involving light-matter interactions such as cavity

quantum electrodynamics and sensing, where the possibility to achieve electric field enhancements in the coupling gap could lead to enhanced interaction cross-sections. Numerical simulations of PMs predict improved properties for label-free biosensing such as an increased sensitivity compared to single microcavities⁵ and the possibility to discriminate—in a self-referenced way—between specific and unspecific binding events,¹⁵ which could make PMs applicable to complex multi-target environments, where unspecific binding events add additional noise to the detection of a specific target.

MATERIALS AND METHODS

Sample fabrication

In order to precisely define the geometry of the PMs and to ensure large-scale production capability and mechanical stability, lithographic fabrication is advantageous compared to common manual arrangement of PMs.^{16–18} Our polymeric, on-chip PM lasers were fabricated by spin-coating a 1.2 μm thick PMMA layer (MicroChem PMMA 950k A6) onto a silicon substrate. To realize active PMs, the laser dye Pyrromethene 597 (Radiant Dyes) was used as gain medium due to its high photostability in polymeric host matrices and high quantum

¹Institute of Applied Physics and DFG Center for Functional Nanostructures CFN, Karlsruhe Institute of Technology, 76128 Karlsruhe, Germany; ²Institute of Microstructure Technology, Karlsruhe Institute of Technology, 76128 Karlsruhe, Germany; ³Institute of Functional Interfaces, Karlsruhe Institute of Technology, 76128 Karlsruhe, Germany and ⁴Carl Zeiss AG, Corporate Research and Technology, 07745 Jena, Germany

Correspondence: Dr T Grossmann, Institute of Applied Physics or Dr T Mappes, Institute of Microstructure Technology, Karlsruhe Institute of Technology (KIT), 76128 Karlsruhe, Germany

E-mail: tobias.grossmann@kit.edu; timo.mappes@kit.edu; URL: www.biophotonic-systems.com

Received 18 September 2012; revised 3 December 2012; accepted 26 February 2013

efficiency.¹⁹ The dye was directly dissolved into the photoresist, resulting in a dye concentration of $25 \mu\text{mol g}^{-1}$ solid content. PMMA microdisks were then patterned by electron beam (e-beam) lithography. After development, the silicon was etched isotropically with XeF_2 , resulting in the microdisks now located on silicon pedestals (Figure 1a). The realization of coupling gaps between two microdisks with well-defined vertical sidewalls is highly limited by the resolution of the fabrication process. The latter is mainly influenced by the e-beam shape and the contrast of the resist. With the given microdisk thickness of $1.2 \mu\text{m}$ the coupling-gap width can be structured lithographically in PMMA as small as 340 nm , corresponding to a microstructure aspect ratio of about 4:1 (inset, Figure 1a). Narrower coupling gaps could allow for significant field enhancements of delocalized (bonding) modes of PMs in the coupling gap—analogueous to the field enhancement in slot waveguides.²⁰ Therefore, a process step was developed, resulting in aspect ratio considerably above the resolution limit of conventional e-beam lithography in thick PMMA resist. Here, an additional $\sim 100 \text{ nm}$ thick layer of poly(*p*-xylylene) (PPX) with a functional alkyne group is conformally polymerized onto the resonators by chemical vapor deposition (Figure 1b). Details of this chemical vapor deposition process step can be found elsewhere.²¹ PPX—often marketed under the name parylene—is transparent in the visible spectral region²² and thus has negligible influence on the threshold of the lasers. With this additional fabrication

step coupling gaps below 150 nm were achieved. Figure 1b shows a scanning electron micrograph of a focused ion beam cut of the coupling region at the minimal distance between two exemplarily chosen microdisks. The aspect ratio of the microstructure with PPX layer is 9:1 with a microdisk thickness of $1.34 \mu\text{m}$ and is thus increased by more than a factor of two compared to the uncoated structure.

Micro-photoluminescence ($\mu\text{-PL}$) spectroscopy

For characterization of the lasing properties of PMs and to analyze the spatial extent of the lasing whispering-gallery modes (WGMs), $\mu\text{-PL}$ spectroscopy was performed. The dye-doped PMs were optically pumped with 10 ns pulses of a frequency doubled Nd:YVO₄ laser at a pump wavelength of 532 nm and a repetition rate of 20 Hz . The pump pulses were focused onto the PM under an incident angle of 45° with respect to the substrate normal using a lens. The pump spot was chosen to have a diameter of approximately $150 \mu\text{m}$ on the sample surface in order to homogeneously pump both microdisks simultaneously. The output emission was collected perpendicular to the PM with a microscope objective ($\text{NA}=0.4$, $20\times$) and either imaged on a CCD-camera (CCD1) or analyzed in a spectrometer (grating with $1200 \text{ lines mm}^{-1}$) equipped with a CCD-camera (CCD2) with an overall spectral resolution of 60 pm (Figure 2a). In addition to spectrally resolving the emission from the sample, the $\mu\text{-PL}$ set-up also resolves the emitted light spatially along the vertical direction, denoted as y -axis in Figure 2b. By aligning the spectrometer entrance slit along the PM's major axis (compare Figure 2b), the emission from a several micrometer wide stripe of the central region of the PM is imaged onto CCD2. This allows for simultaneous recording of the WGM-lasing from both ends of the PM as well as from the coupling gap, resulting in separated lasing spectra on CCD2.

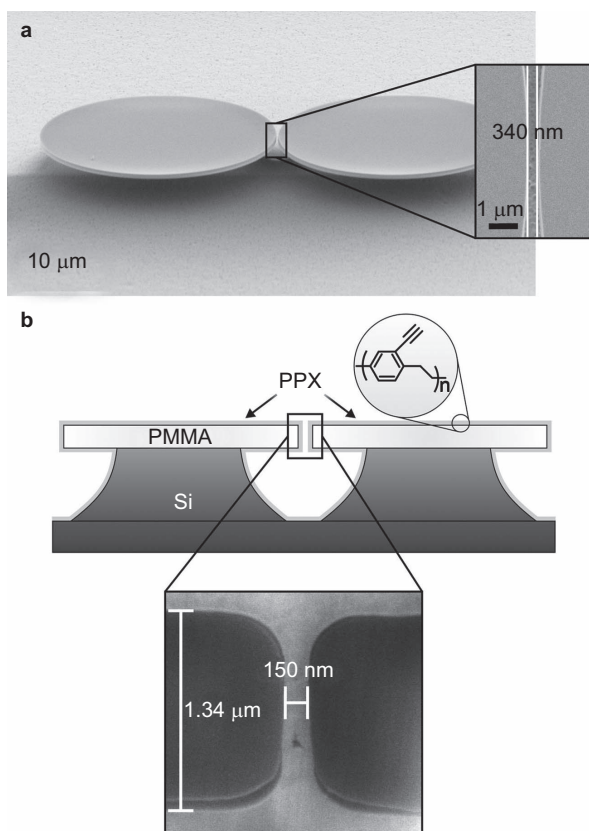


Figure 1 (a) Scanning electron micrograph of a photonic molecule consisting of two coupled microdisk resonators with radii of each $25 \mu\text{m}$ and a coupling-gap width of 340 nm structured by e-beam lithography, standing on silicon pedestals. (b) Deposition of an additional layer of PPX after the lithographic structuring can significantly decrease the coupling-gap width below 150 nm . The inset shows a scanning electron micrograph of the cross-section of the coupling region at the minimal distance between the microdisks fabricated by a focused ion beam cut. PPX, poly(*p*-xylylene).

RESULTS AND DISCUSSION

To determine the coupling-dependent properties of the PM lasers, size-mismatched cavities with radii of 20 and $25 \mu\text{m}$ and coupling-gap widths varying from 0 to 200 nm in steps of about 25 nm were investigated. The spatially resolved lasing spectra of the coupled microcavity lasers with a coupling gap of around 200 nm are depicted in Figure 2b, where the sample was pumped with an energy of 30 nJ per pulse. A comparison of the lasing spectra from both ends of the PM in Figure 2b clearly shows that both microcavities support different lasing modes with differing gain spectra (marked by dashed rectangles) and differing cavity modes. Two examples of cavity modes which are localized in solely one of the microdisks are marked by solid white rectangles in Figure 2b. These lasing modes with high intensity in one cavity only show weak photoluminescence intensity in the other cavity. Despite optical coupling between the resonators, no significant field build-up in the other microdisk occurs. This can be attributed to the different cavity sizes and hence differing resonance wavelengths of both resonators. The weak coupling to the other resonator can therefore be considered as an additional loss mechanism. Decreasing the coupling-gap width leads to an increase of coupling loss and hence to a decrease of the Q factor of the WGMs. This causes an increase of the lasing thresholds which is expected to lead to suppression of modes and is often referred to as Vernier effect.^{13,14} A quantitative analysis of the suppression of lasing modes of the PMs was performed by counting the total number of laser modes in the spectrum acquired by pumping PMs with coupling gaps varying from 0 to 200 nm with an energy of 30 nJ . These PMs with varying coupling-gap widths were all fabricated on a single substrate. The effect of a decreasing coupling gap on the number of lasing modes of the PM is

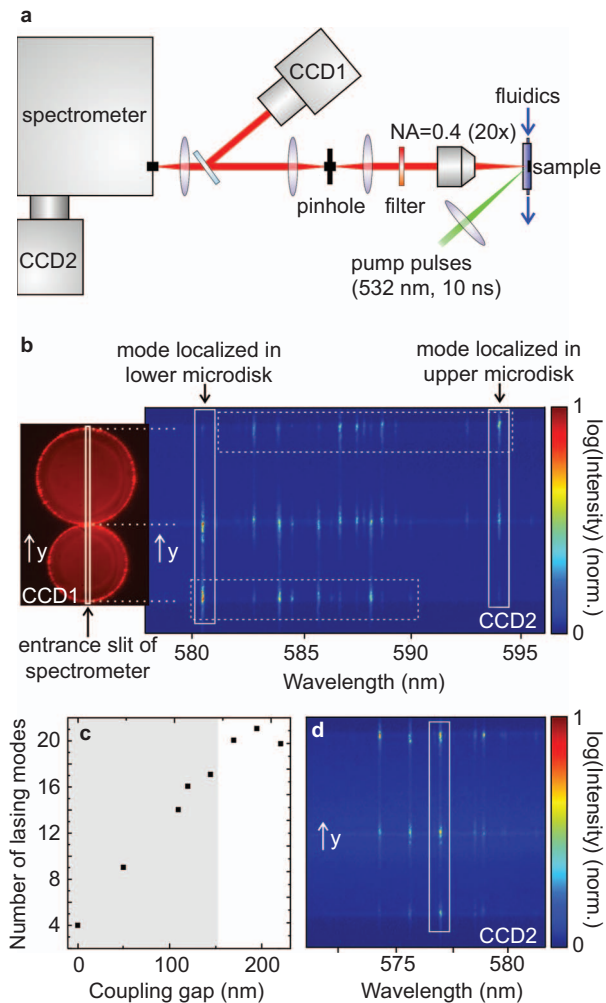


Figure 2 (a) The experimental setup for the investigation of PM lasing modes. The CCD camera CCD1 is used for the two-dimensional imaging of the spectrally integrated photoluminescence. CCD2 detects the spectrally resolved photoluminescence with a spatial resolution in the vertical dimension. (b) Images made by both CCDs of the lasing WGMs in size-mismatched PMs with a coupling gap of 200 nm. The emitted lasing spectra of both cavities vary due to their different size (disk radii: 20 and 25 μm) and weak inter-cavity coupling. The modes are localized in either of the cavities. The unequal spacing of the modes originates from mode competition in the presence of gain in the active microcavities. (c) The number of lasing modes is significantly decreased for coupling-gap widths below 150 nm. (d) Section of the lasing spectrum of a PM with a coupling gap of 120 nm, showing that for increased intra-cavity coupling delocalized lasing modes (marked by a solid white rectangle) exist. PM, photonic molecule; WGM, whispering-gallery mode.

depicted in Figure 2c, where the number of lasing modes includes the modes of both microdisks. For coupling-gap widths above 150 nm, the number of lasing modes is almost constant and no suppression of laser modes can be observed. Below 150 nm, a significant decrease in the number of lasing modes was observed. Comparing the number of modes for the largest and smallest coupling-gap width shows a decrease up to a factor of five. This indicates that efficient suppression of laser modes in size-mismatched cavities only occurs above a certain coupling strength and seems to have a threshold-like behavior. This observation can be explained by considering the degree of coupling between the resonators, which can be analyzed analytically by calculation of the coupling constant κ . An analytic expression for calculation of κ was presented by Little *et al.*²³ The coupling constant was found

to increase monotonically for decreasing coupling-gap size. For the size-mismatched PMs investigated in this work (microdisks with radii of 25 and 20 μm and a resonance wavelength of 580 nm), the coupling constant was found to take on values significantly above zero for coupling-gap widths smaller than 300 nm. This is consistent with the above discussed observation of weak photoluminescence of the modes, which are mainly localized in one of the resonators, in the other cavity (compare Figure 2b). For values of the coupling-gap width below 150 nm, the coupling constant takes on values above 0.03. This value of κ seems to be a threshold value where the losses induced by coupling become dominant compared to the other loss mechanisms of the modes, such as surface scattering losses. The Vernier effect observed in the PMs presented in this work therefore only occurs for coupling-gap widths below 150 nm.

Besides a reduced number of modes, lasing modes with equal intensities at both ends of the PM were observed for coupling-gap widths smaller than 150 nm. An example for this case is depicted in Figure 2d, where the coupling-gap width of the size-mismatched PM is 120 nm. Here, a lasing mode (marked by a solid white rectangle) with high relative intensities in both cavities was observed and can thus be considered as delocalized super-mode which extends over both resonators and arises from the strong optical coupling between the two microdisks. This is therefore consistent with the observation of enhanced lasing mode suppression in this regime, where the number of lasing modes is about a factor five lower compared to regime of weaker coupling. For delocalized modes, the inter-cavity coupling does not lead to additional losses, as both resonators support the same resonance wavelength. Therefore, delocalized lasing modes were found to have a lower threshold compared to localized modes due to the absence of coupling losses.

In addition to the above presented operation of PM lasers in air, lasing properties were investigated in aqueous environment to demonstrate the potential use of these devices for sensing applications. The reduced refractive index contrast between cavity and aqueous solution has the advantage that less-confined modes, such as higher order radial modes of the microdisks, have a lower Q factor and higher lasing threshold due to increased radiation losses. Therefore, these modes do not contribute to lasing oscillations at moderate pump powers and the overall number of lasing modes is reduced compared to the situation in air. Furthermore, the evanescent fields of the WGMs are extended further into the aqueous medium leading to a stronger coupling between the resonators. In water, this results in delocalized lasing modes for coupling-gap widths already from 300 nm and below. Furthermore, pronounced single-mode lasing could be achieved. A lasing spectrum showing single-mode operation is depicted in Figure 3a, recorded at a pump energy of 84 nJ. The single-mode lasing was observed in a PM with a coupling-gap width of around 250 nm. The single-mode lasing was still apparent at higher pump energies, indicating a very efficient suppression of lasing modes. The inset of Figure 3a depicts a lasing spectrum at a pump energy of 215 nJ, which is more than three times the value of the lasing threshold of 65 nJ, determined from the input-output characteristics of the laser mode at 579 nm (Figure 3b). Although several side modes appeared at high pump energies, the intensity of the dominating lasing mode was still more than six times higher than the most intense side mode. This indicates that almost all pump energy is transferred into the dominating mode due to the effective suppression of side modes.

CONCLUSIONS

In summary, we presented a method which allows for the fabrication of on-chip WGM PMs with coupling-gap widths below 150 nm by

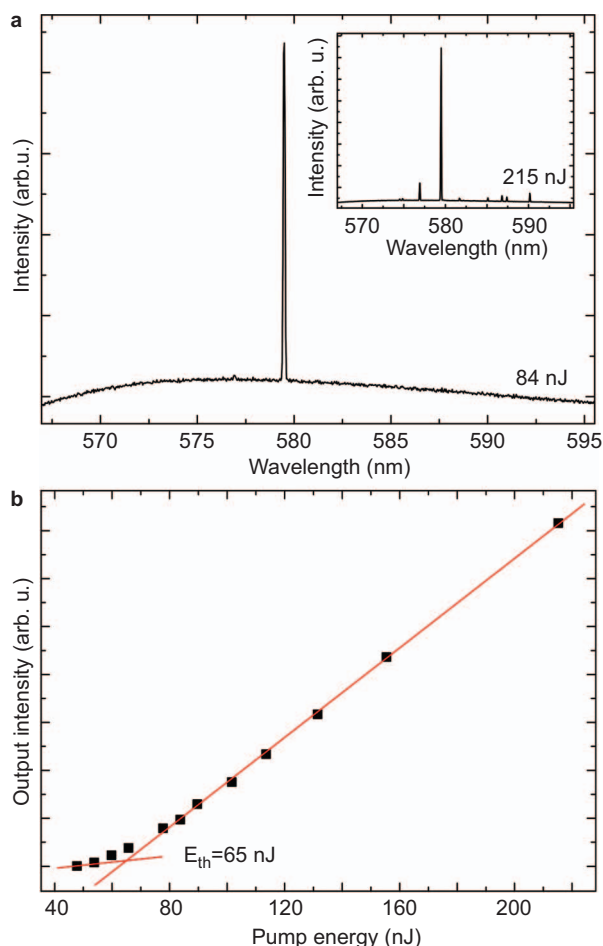


Figure 3 (a) Single-mode lasing from size-mismatched PMs in aqueous environment. (b) The lasing threshold for the laser mode is around 65 nJ. The coupling-gap width of the PM in this case was around 250 nm. PM, photonic molecule.

combining lithography with the subsequent deposition of an additional PPX polymer layer *via* chemical vapor deposition. In order to resolve the spatial distribution of lasing WGMs, μ -PL spectroscopy was used to determine the localization of the modes. By varying the coupling-gap width between size-mismatched microdisks, we determined that suppression of laser modes only occurs above a certain coupling strength and showed a threshold like behavior. In the regime of strong optical coupling, we observe super-modes which are delocalized in both microcavities. Furthermore, the PMs were operated in aqueous environments, where they showed distinctive single-mode lasing even at pump powers well above the lasing threshold.

The presented lithographic fabrication method for PMs could allow for realization of large arrays of strongly coupled, on-chip cavities with precisely defined coupling-gap sizes, which is of great interest for applications in quantum optics. The additional PPX layer not only reduces the coupling gaps, but also provides chemical end-groups on the PM surface and the surrounding silicon and can thus serve as starting layer for the surface functionalization for the label-free detection of target molecules as well as for solventless adhesive bonding of additional microfluidic elements onto the silicon substrate, making our presented approach highly interesting for the realization of integrated optofluidic devices.

ACKNOWLEDGMENTS

The authors gratefully acknowledge technical support from Patrice Brenner (CFN, KIT) during focused ion beam cuts and Peter-Juergen Jakobs and Andreas Bacher (both IMT, KIT) during e-beam lithography. This work has been supported by the DFG Research Center for Functional Nanostructures (CFN) Karlsruhe, by a grant from the Ministry of Science, Research, and the Arts of Baden-Württemberg (Grant No. Az:7713.14-300) and by the German Federal Ministry for Education and Research BMBF (Grant No. FKZ 13N8168A). This work was partly carried out with the support of the Karlsruhe Nano Micro Facility (KNMF), a Helmholtz Research Infrastructure at KIT. TG gratefully acknowledges financial support of the Deutsche Telekom Stiftung and the Karlsruhe House of Young Scientists (KHYS). The authors thank the Karlsruhe School of Optics and Photonics (KSOP) for continuous support.

- 1 Skarja M, Borštnik NM, Löffler M, Walther H. Quantum interference and atom-atom entanglement in a two-mode, two-cavity micromaser. *Phys Rev A* 1999; **60**: 3229–3232.
- 2 Bose S, Angelakis DG, Burgarth D. Transfer of a polaritonic qubit through a coupled cavity array. *J Mod Opt* 2007; **54**: 2307–2314.
- 3 Hartmann MJ, Brandão FG, Plenio MB. Effective spin systems in coupled microcavities. *Phys Rev Lett* 2007; **99**: 160501.
- 4 Hartmann MJ, Brandão FG, Plenio MB. Quantum many-body phenomena in coupled cavity arrays. *Laser Photon Rev* 2008; **2**: 527–556.
- 5 Boriskina SV. Spectrally engineered photonic molecules as optical sensors with enhanced sensitivity: a proposal and numerical analysis. *J Opt Soc Am B* 2006; **23**: 1565–1573.
- 6 Peng C, Li Z, Xu A. Optical gyroscope based on a coupled resonator with the all-optical analogous property of electromagnetically induced transparency. *Opt Express* 2007; **15**: 3864–3875.
- 7 Lu TW, Lee PT. Ultra-high sensitivity optical stress sensor based on double-layered photonic crystal microcavity. *Opt Express* 2009; **17**: 1518–1526.
- 8 Guzatov DV, Woggon U. Coupled microsphere clusters for detecting molecule's dipole moment orientation. *Appl Phys Lett* 2009; **94**: 241104.
- 9 Zhang X, Ren L, Wu X, Li H, Liu L *et al*. Coupled optofluidic ring laser for ultrahigh-sensitive sensing. *Opt Express* 2011; **19**: 22242–22247.
- 10 Hryniewicz JV, Absil PP, Little BE, Wilson RA, Ho PT. Higher order filter response in coupled microring resonators. *IEEE Photon Technol Lett* 2000; **12**: 320–322.
- 11 Savchenkov AA, Ilchenko VS, Matsko AB, Maleki L. High-order tunable filters based on a chain of coupled crystalline whispering gallery-mode resonators. *IEEE Photon Technol Lett* 2005; **17**: 136–138.
- 12 Bayer M, Gutbrod T, Reithmaier JP, Forchel A, Reinecke TL *et al*. Optical modes in photonic molecules. *Phys Rev Lett* 1998; **81**: 2582–2585.
- 13 Lee W, Li H, Suter JD, Reddy K, Sun Y *et al*. Tunable single mode lasing from an on-chip optofluidic ring resonator laser. *Appl Phys Lett* 2011; **98**: 061103.
- 14 Shang L, Liu L, Xu L. Single-frequency coupled asymmetric microcavity laser. *Opt Lett* 2008; **33**: 1150–1152.
- 15 Boriskina SV, Dal Negro L. Self-referenced photonic molecule bio (chemical) sensor. *Opt Lett* 2010; **35**: 2496–2498.
- 16 Shang L, Liu L, Xu L. Highly collimated laser emission from a peanut-shaped microcavity. *Appl Phys Lett* 2008; **92**: 071111.
- 17 Möller B, Woggon U, Artemyev M, Wannemacher R. Photonic molecules doped with semiconductor nanocrystals. *Phys Rev B* 2004; **70**: 1–5.
- 18 Lin H, Chen JH, Chao SS, Lo MC, Lin SD *et al*. Strong coupling of different cavity modes in photonic molecules formed by two adjacent microdisk microcavities. *Opt Express* 2010; **18**: 23948–23956.
- 19 Bañuelos Prieto J, López Arbeloa F, Martínez Martínez V, Arbeloa López T, López Arbeloa I. Photophysical properties of the pyromethene 597 dye: solvent effect. *J Phys Chem A* 2004; **108**: 5503–5508.
- 20 Leuthold J, Koos C, Freude W. Nonlinear silicon photonics. *Nat Photon* 2010; **4**: 535–544.
- 21 Chen HY, Lahann J. Designable biointerfaces using vapor-based reactive polymers. *Langmuir* 2011; **27**: 34–48.
- 22 Szentesi OI, Noga EA. Parylene C films for optical waveguides. *Appl Opt* 1974; **13**: 2458–2459.
- 23 Little B, Chu S, Haus H, Foresi J, Laine JP. Microring resonator channel dropping filters. *J Lightwave Technol* 1997; **15**: 998–1005.



This work is licensed under a Creative Commons Attribution-NonCommercial-NoDerivative Works 3.0 Unported License. To view a copy of this license, visit <http://creativecommons.org/licenses/by-nc-nd/3.0>